

BISATIC SAR SLC IMAGE MODELLING AND INTERFEROMERIC GENERATION

Dimitar Minchev, Andon Lazarov

Burgas Free University, Faculty of Computer Science and Engineering, Burgas, Bulgaria
mitko@bfu.bg, lazarov@bfu.bg

Keywords: SAR, InSAR, BInSAR, LFM, SLC, Signal Model, Image Modelling, Interferogram generation.

Abstract: This work addresses the model of Bistatic Interferometric Synthetic Aperture Radar BInSAR imaging process. BInSAR geometry with multiple satellite receivers is thoroughly mathematical described. A linear frequency modulated (LFM) SAR signal model and single look complex (SLC) image are derived. To verify proposed models an implementation of the processing chain, implemented in MATLAB environment is performed.

1 INTRODUCTION

Imaging capability of Synthetic Aperture Radar (SAR) Distributed Satellite-borne Systems (DSS) with Bistatic Interferometric Synthetic Aperture Radar (BInSAR) on board is already proven Earth Remote Sensing technique. BInSAR DSS system error analysis and design method are investigated in (Li Wei, 2002). The potential benefits, drawbacks and problems associated with a close formation flight for an along-track interferometry SAR mission is discussed in (Eberhard, 2004). A generalized approach of formation configuration of BInSAR DDS from the point of system performance optimization is presented in (Huang, 2007). Concept for decomposition of solid baseline, a new method to avoid the max detection error and simulation experiment accompanied by very good result is shown in (Xilong, 2007). Effective method to eliminate the effect of baseline instability on SAR image and interferometric measure is proposed in (Zhang, 2007). A multi-baseline polarimetric synthetic aperture radar interferometry (Pol-InSAR) technique that allows more appropriate reconstruction of the quasi-three-dimensional spatial distribution of scattering processes within natural media is presented in (Stebler, 2002).

The main purpose of this work is to propose a universal geometrical model of the Earth surface topography, as well as mathematical model of the reflected LFM SAR signals from that relief and

algorithms for complex image extraction and interferogram generation.

2 GEOMETRY AND KINEMATICS OF SAR SCENARIO

Consider Bistatic Interferometric Synthetic Aperture Radar (BInSAR) geometry (Fig.1), defined in coordinate system $Oxyz$. SAR system is located on a satellite with a trajectory given by the following vector equation.

$$\mathbf{R}(p) = \mathbf{R}_0 + \mathbf{V}T_p\left(\frac{N}{2} - p\right) \quad (1)$$

where: $\mathbf{R}_0 = \mathbf{R}(0)$ is the distance vector from the origin of the coordinate system to the satellite in the moment $t = 0$; \mathbf{V} is the satellite velocity vector; T_p is the signal repetition period; p is the index of emitted pulses; N is the full number of emitted pulses. The vector equation (1) is projected in coordinate system $Oxyz$, which yields

$$\begin{aligned} x(p) &= x_0 - V_x T_p \left(\frac{N}{2} - p\right) \\ y(p) &= y_0 - V_y T_p \left(\frac{N}{2} - p\right) \\ z(p) &= z_0 - V_z T_p \left(\frac{N}{2} - p\right) \end{aligned} \quad (2)$$

where $x(p)$, $y(p)$ and $z(p)$ are the satellite coordinates in the moment p ; $x_0 = x(0)$, $y_0 = y(0)$ and $z_0 = z(0)$ are the satellite coordinates in the moment $p = N/2$; $V_x = V \cos \alpha$, $V_y = V \cos \beta$, $V_z = V \cos \delta$ are coordinates of the velocity vector; $\cos \alpha$, $\cos \beta$, $\cos \beta$ are the guiding cosines of the velocity vector.

The surface depicted in coordinate system $Oxyz$ analytically can be presented as a two dimensional function, i.e. z as a function of coordinates x and y , which in discrete form is given by the following equation (3)

$$\begin{aligned} z_{mn} = z_{mn}(x_{mn}, y_{mn}) = & \\ 3(1 - x_{mn})^2 \exp[-(x_{mn})^2 - (y_{mn} + 1)^2] & \\ - 10 \left(\frac{x_{mn}}{5} - x_{mn}^3 - y_{mn}^5 \right) \exp[x_{mn}^2 - y_{mn}^2] & \quad (3) \\ - \frac{1}{3} \exp[-(x_{mn} + 1)^2 - y_{mn}^2] & \end{aligned}$$

where $x_{mn} = m\Delta M$ and $y_{mn} = n\Delta N$ are discrete coordinates in the plane Oxy ; ΔM and ΔN are dimensions of the grid's cell; m and n - relative discrete coordinates (*indexes*) on axes Ox and Oy . Coordinates; x_{mn} , y_{mn} and z_{mn} define the distance vector \mathbf{R}_{mn} of each point scatterer.

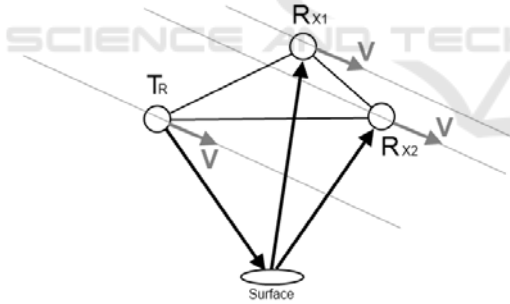


Figure 1: Bistatic InSAR Geometry.

Assume that in each grid's cell with dimensions (ΔM and ΔN) and coordinates (x_{mn} , y_{mn}) one prominent point scatterer is located. During the process of observation the distance vector $\mathbf{R}_{mn}(p)$ from SAR located on the satellite to the dominant point scatterer, defined by the geometrical vector \mathbf{R}_{mn} , can be expressed by the following vector equation

$$\mathbf{R}_{mn}(p) = \mathbf{R}(p) - \mathbf{R}_{mn} \quad (4)$$

The geometry information of the observed surface is contained in the phase of the complex amplitude of

the reflected signal from each point scatterer which is proportional to the module of the distance vector $R_{mn}(p)$ defined by the expression

$$R_{mn}(p) = \sqrt{[x(p) - x_{mn}]^2 + [y(p) - y_{mn}]^2 + [z(p) - z_{mn}]^2} \quad (5)$$

While modelling the process of observation the value of the parameter $R_{mn}(p)$ is calculated for each p , m and n .

3 LFM SAR SIGNAL MODELING AND SLC IMAGE RECONSTRUCTION

3.1 SAR signal modelling algorithm

1. Compute the distance from SAR to each point scatterer from the observed surface for each particular moment p by equation (5).
2. Compute time delay parameter for each point scatterer from the surface $t_{mn}(p)$ by the expression

$$t_{mn}(p) = \frac{R_{mn}^{TR}(p) + R_{mn}^{RX1}(p)}{c} \quad (6)$$

where $c = 3.10^8$ m/s is the speed of light, R_{mn}^{TR} is the distance from transmitter to the surface; R_{mn}^{RX1} is the distance from the surface to the receiver satellite.

3. Compose an one-dimensional array with entities of all time delays $t_{mn}(p)$ arranged in ascending order and define minimum $t_{mn \min}(p)$.

4. Compute generalized time parameter of the reflected signal:

$$E_{mn}(k, p) = t_{mn \min}(p) + (k - 1)\Delta T - t_{mn}(p) \quad (7)$$

5. Compute LFM signal, reflected by mn -th point scatterer for each sample $k = \{1, 2, \dots, 256\}$ and emitted pulse $p = \{1, 2, \dots, 256\}$.

$$S_{mn}(k, p) = a_{mn} \cdot \exp\left\{j\left[\omega E_{mn}(k, p) + b(E_{mn}(k, p))^2\right]\right\} \quad (8)$$

6. The results of the computation of are placed in a two dimensional array $[k, p]$.

The SAR signal, reflected from a particular point scatterer is limited within pulse duration, which can be described by element wise multiplication of the signal $S_{mn}(k, p)$ (8) with a rectangular function i.e.

$$S_{mn, \text{rect}}(k, p) = \text{rect}\left(\frac{E}{T_k}\right) \cdot S_{mn}(k, p) \quad (9)$$

where

$$\text{rect}\left(\frac{E}{T_k}\right) = \begin{cases} 1, 0 \leq \frac{E}{T_k} < 1 \\ 0, \frac{E}{T_k} < 0, \frac{E}{T_k} \geq 1 \end{cases} \quad (10)$$

is the rectangular function described by two dimensional matrix $[k, p]$, containing zeros and ones in positions according to conditions (10).

The element wise multiplication of the matrix $S_{mn}(k, p)$ with rectangular matrix function

$\text{rect}\left(\frac{E}{T_k}\right)$ yields a matrix $S_{mn,\text{rect}}(k, p)$, which

contains all necessary values of the SAR, reflected by particular point scatterer. Superposition of reflected SAR signals over dimensions m and n yields the values of the interferon complex SAR signal $S(k, p)$, written as entities of a two dimensional matrix $[p, k]$, i.e.

$$S(k, p) = \sum_{m=1}^M \sum_{n=1}^N S_{mn,\text{rect}}(k, p) \quad (11)$$

3.2 SAR SLC image reconstruction

1. Demodulation of the SAR signal by multiplication of two dimensional matrix $S(k, p)$ with complex conjugated emitted signal, i.e.

$$\tilde{S}(k, p) = S(k, p) \cdot \exp\left\{j\left[\omega(k-1)\Delta T + b((k-1)\Delta T)^2\right]\right\} \quad (12)$$

2. SLC image reconstruction by standard two dimensional fast Fourier transform

$$\hat{I}(\bar{k}, \bar{p}) = \text{FFT}_p[\text{FFT}_k(\tilde{S}(k, p))] \quad (13)$$

The matrix $\hat{I}(\bar{k}, \bar{p})$ represents the complex image of the observed surface, containing amplitude and phase information for each pixel from the surface.

In Fig. 2 real (a) and imaginary (b) parts of the complex SAR signal are presented.

3.3 Interferogram generation

An interferogram is generated by complex conjugate multiplication of obtained two Single Look Complex (SLC) images.

4 NUMERICAL EXPERIMENT

Distributed Satellite-borne Systems (DSS) with Bistatic Interferometric Synthetic Aperture Radar (BInSAR), formed by three SAR satellite systems observe Earth surface which is modelled by Matlab “peaks” function. T_R is the transmit satellite, while

R_{X1} and R_{X2} are receiver satellites. Satellites’ trajectory parameters and SAR data are presented in Table 1.

Table 1: Trajectory and SAR parameters.

	T_R	R_{X1}	R_{X2}
x_0	$2 \cdot 10^4$	10^4	$1,2 \cdot 10^4$
y_0	$2 \cdot 10^4$	10^4	10^4
z_0	$8 \cdot 10^5$	$8 \cdot 10^5$	$8 \cdot 10^5$
N_p	512	512	512
N_k	512	512	512
m_n	256	256	256
Δ	2	2	2
$V(\text{m/s})$	1000	1000	1000
T_p (s)	0.025	0.025	0.025
T_k (s)	0.0025	0.0025	0.0025
F (Hz)	10^{10}	10^{10}	10^{10}
ΔF (Hz)	$2,5 \cdot 10^7$	$2,5 \cdot 10^7$	$2,5 \cdot 10^7$

Baseline between T_R and R_{X1} is $10^4 \cdot \sqrt{2} = 14142,136$ meters. Baseline between T_R and R_{X2} is 12806,248 meters. Baseline between R_{X1} and R_{X2} is 2000 meters. Computational results are shown in Figs. 2-6.

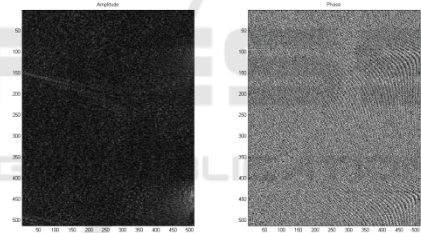


Figure 2: SAR1 SLC image

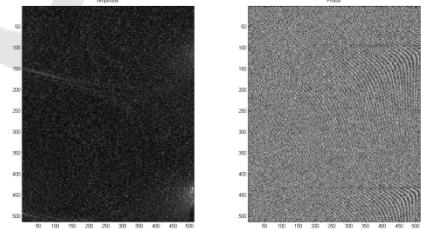


Figure 3: SAR2 SLC image

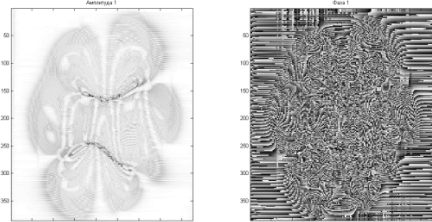


Figure 4: Reconstructed RX1 SAR image (amplitude and phase)

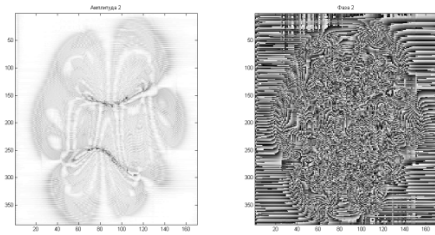


Figure 5: Reconstructed RX2 SAR image (amplitude and phase)

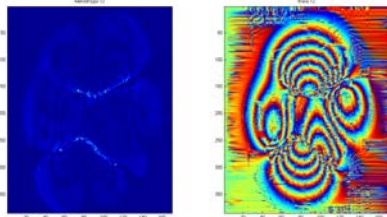


Figure 6: Interferometric phase based on RX1 SLC image and RX2 SLC image

In Fig. 6 clearly can be seen interferometric fringes proportional to heights and depths of the observed surface.

5 CONCLUSION

In this work a model of Bistatic Interferometric Synthetic Aperture Radar (BInSAR) imaging process is discussed. Bistatic InSAR geometry with thoroughly mathematical description of the observed surface and kinematic equations is suggested. LFM SAR signal's model is derived. SLC image reconstruction algorithm with two dimensional FFT procedures is implemented. To verify proposed geometrical and signal models a simulation of the processing chain, implemented in MATLAB environment is illustrated. SAR complex interferogram containing amplitude and phase information is produced.

ACKNOWLEDGEMENTS

This work is supported by NATO ESP.EAP.CLG. 983876 and MEYS, Bulgarian Science Fund the project DTK 02/28.2009, DDVU 02/50/2010.

REFERENCES

- Li Wei, Li Chunsheng, 2002. A novel system parameters design and performance analysis method for Distributed Satellite-borne SAR system, *Advances in Space Research*, Volume 50, Issue 2, 15 July 2012, Pages 272-281, ISSN 0273-1177, 10.1016 /j.asr.2012.03.026, <http://www.sciencedirect.com/science/article/pii/S0273117712002244>
- Xilong, S., Anxi, Y., Zhen, D., Diannong, L., 2007. Research on differential interferometry for spaceborne bistatic SAR, (2007) *International Geoscience and Remote Sensing Symposium (IGARSS)*, art. no. 4423252, pp. 2118-2121., <http://www.scopus.com/inward/record.url?eid=2-s2.0-82355161233&partnerID=40&md5=5834d01988df2fdd978780e3d16301a>
- O Stebler, E Meier, D Nüesch, 2002. Multi-baseline polarimetric SAR interferometry—first experimental spaceborne and airborne results, *ISPRS Journal of Photogrammetry and Remote Sensing*, Volume 56, Issue 3, April 2002, Pages 149-166, ISSN 0924-2716, 10.1016/S0924-2716(01)00049-1, <http://www.sciencedirect.com/science/article/pii/S0924271601000491>
- Zhang, Q.-L., Lu, Y.-B. 2007. The study on imaging algorithm of formation flying satellites InSAR system, 2007 1st Asian and Pacific Conference on Synthetic Aperture Radar Proceedings, APSAR 2007, art. no. 4418547, pp. 27-31., <http://www.scopus.com/inward/record.url?eid=2-s2.0-47349123731&partnerID=40&md5=ade1b6b133e46f02bc5116b25b012cac>
- Huang, H., Liang, D., 2007. Optimization design approach of distributed spaceborne InSAR formation, *Hangkong Xuebao/Acta Aeronautica et Astronautica Sinica*, 28 (5), pp. 1168-1174., <http://www.scopus.com/inward/record.url?eid=2-s2.0-35348988096&partnerID=40&md5=6e9eb60a36628c5d67a06ebf58346dec>
- Eberhard Gill, Hartmut Runge, 2004. Tight formation flying for an along-track SAR interferometer, *Acta Astronautica*, Volume 55, Issues 3–9, August–November 2004, Pages 473-485, ISSN 0094-5765, 10.1016/j.actaastro.2004.05.044., <http://www.sciencedirect.com/science/article/pii/S0094576504001870>